Atmos. Chem. Phys. Discuss., 12, 15049–15082, 2012
www.atmos-chem-phys-discuss.net/12/15049/2012/
doi:10.5194/acpd-12-15049-2012

Atmospheric Chemistry and Physics Discussions

Process analysis of regional ozone formation over the Yangtze River Delta, China using the Community Multi-scale Air Quality modeling system

L. Li[1], C. H. Chen[1], C. Huang[1], H. Y. Huang[1], G. F. Zhang[1], Y. J. Wang[2], H. L. Wang[1], S. R. Lou[1], L. P. Qiao[1], M. Zhou[1], M. H. Chen[1], Y. R. Chen[1], J. S. Fu[3], D. G. Streets[4], and C. J. Jang[5]

[1]Shanghai Academy of Environmental Sciences, Shanghai, 200233, China
[2]Institute of Environmental Pollution and Health, School of Environmental and Chemical Engineering, Shanghai University, Shanghai 200444, China
[3]Department of Civil & Environmental Engineering, University of Tennessee, Knoxville, TN 37996, USA
[4]Decision and Information Sciences Division, Argonne National Laboratory, Argonne, IL 60439, USA
[5]Office of Air Quality Planning & Standards, US Environmental Protection Agency, Research Triangle Park, NC 27711, USA

Received: 20 April 2012 – Accepted: 25 May 2012 – Published: 13 June 2012

Correspondence to: C. H. Chen (chench@saes.sh.cn)

Published by Copernicus Publications on behalf of the European Geosciences Union.

ACPD

12, 15049–15082, 2012

Abstract

High ozone concentration has become an important issue in summer in most economically developed cities in Eastern China. In this paper, observations at an urban site within the Shanghai city are used to examine the typical high ozone episodes in August 2010, and the MM5-CMAQ modeling system is then applied to reproduce the typical high ozone episodes. In order to account for the contribution of different atmospheric processes during the high pollution episodes, the CMAQ integrated process rate (IPR) is used to assess the different atmospheric dynamics in rural and urban sites of Shanghai, Nanjing and Hangzhou, which are typical cities of the Yangtze River Delta (YRD) region. In order to study the contributions of the main atmospheric processes leading to ozone formation, vertical process analysis in layer 1 (0–40 m), layer 7 (350–500 m), layer 8 (500–900 m) and layer 10 (1400–2000 m) has been considered. The observations compare well with the results of the numerical model. IPR analysis shows that the maximum concentration of ozone occurs due to transport phenomena, including vertical diffusion and horizontal advective transport. The gas-phase chemistry producing O_3 mainly occurs in the height of 300–1500 m, causing a strong vertical O_3 transport from upper levels to the surface layer. The gas-phase chemistry is an important sink for O_3 in the surface layer, coupled with dry deposition. The cloud processes, horizontal diffusion and heterogeneous chemistry contributions are negligible during the whole episode. In the urban Shanghai area, the average O_3 production rates contributed by vertical diffusion and horizontal transport are 24.7 ppb h^{-1}, 3.6 ppb h^{-1}, accounting for 27.6 % and 6.6 % of net surface O_3 change, respectively. The average contributions of chemistry, dry deposition and vertical advective transport to O_3 production are −21.9, −4.3 and −2.1 ppb h^{-1}, accounting for −25.3 %, −5.0 % and −3.7 % of net O_3 change, respectively. In the suburban and industrial areas of Shanghai, net transport accounts for 26.3 % and chemical reaction for −11.1 % of net surface O_3 change. At the Nanjing site, the net transport accounts for 9 % and chemical reaction for −32 %. However, at the heights of 350–500 m and 500–900 m, during the time period of 10:00–15:00 LST,

ACPD
12, 15049–15082, 2012

photochemistry plays the most important role in net O_3 production, with the highest positive contributions from gas-phase chemistry to net O_3 production reaching 87.3 % and 68.6 %, respectively, and making a strong vertical O_3 transport from upper levels to the surface layer. At the Hangzhou site, the net transport accounts for 9 % and chemical reaction for −9 % of the net O_3 change. Modeling results show that the O_3 pollution characteristics among the different cities in the YRD region have both similarities and differences. During the buildup period (usually from 08:00 in the morning after sunrise), the O_3 starts to appear in the city regions like Shanghai, Hangzhou, Ningbo and Nanjing and is then transported to the surrounding areas under the prevailing wind conditions. The O_3 production from photochemical reaction in Shanghai and the surrounding area are most significant, due to the high emission intensity in the large city; this ozone is then transported out to sea by the westerly wind flow, and later diffuses to rural areas like Chongming island, Wuxi and even to Nanjing. The O_3 concentrations start to decrease in the cities after sunset, due to titration of the NO emissions, but ozone can still be transported and maintain a significant concentration in rural areas and even regions outside the YRD region, where the NO emissions are very small.

1 Introduction

With the rapid economic development and significant increase of energy consumption, the anthropogenic emissions have been continuously growing in recent years in Eastern China, which have led to significant changes in atmospheric ozone, including the increase in tropospheric ozone. More and more concerns have been focused on the regional pollution in those leading economic regions, for example, the Yangtze River delta (Zhao et al., 2004; Wang et al., 2005; Li et al., 2011), the Pearl River delta (Wang et al., 2010; Shen et al., 2011), and the Bohai Bay region (Wang et al., 2006, 2009, 2010; An et al., 2007; Chou et al., 2011). In recent years, high ozone concentrations over 90 ppb have been frequently observed by in-situ monitoring in Eastern China (Zhang et al., 2008; Ran et al., 2009; Shao et al., 2009; Tang et al., 2009). In many megacities

ACPD
12, 15049–15082, 2012

and polluted areas in Eastern China, serious ozone pollution caused by large precursor emissions has concerned citizens and decision-makers (Shao et al., 2009).

Ozone originates from in-situ photochemical production in the reactions from the mixture of reactive volatile organic compounds (VOCs) and nitrogen oxides (NO_x) and from vertical and horizontal transport. In the troposphere, photolysis of ozone by solar UV radiation to electronically excited $O(^1D)$ and the subsequent reaction with water vapor is the major source of hydroxyl radical (OH). OH is one of the key species for the chemical reactions in the atmosphere and its abundance is an important index of the oxidizing capacity of the atmosphere. Thus, the control of O_3 is a complicated problem due to the nature of the non-linear formation of O_3 (Seinfeld and Pandis, 2006).

The Yangtze River Delta (YRD), characterized by high population density and well-developed industry, is one of the largest economic regions in China. Many studies related to the ozone concentration in the YRD have been conducted in the past years. Observations made by Xu et al. (2006) show that high ozone concentrations in the YRD have occurred. Xu et al. (2007) analyzed the tropospheric ozone using satellite data and found that the tropospheric ozone concentration has kept on increasing in the YRD. Especially, Chan and Yao (2008) have given a general review on the ozone mass concentrations and formation studies done in Shanghai, a typical mega city in the YRD, showing that some O3 episodes have occurred in the region. However, since the YRD is a large area, the emissions rates and emission characteristics of the ozone precursors vary greatly. This means that the ozone formation process differs with areas in the region. Studies on the process analysis of typical ozone episodes over the YRD are quite limited up to now.

In this study, we first perform an observation analysis to identify a typical summertime O_3 episode over the YRD in 2010. Then the Community Multi-scale Air Quality Modeling System (CMAQ) (Dennis et al., 1996; Byun et al., 1998; Byun and Ching, 1999) is used to reproduce the high ozone case, and integrated process rate analysis (IPR), implemented within CMAQ, is applied to analyze the formation of ozone at typical sites in the YRD. This is undertaken to identify the dominant processes contributing

ACPD
12, 15049–15082, 2012

to the O_3 formation and determine the characteristics of the photochemical system at different locations or at a given location on different days.

2 Methodology

2.1 Model setup and input data

In this paper, the CMAQ version 4.6 is used with the Carbon Bond 05 (CB05) chemical mechanism to simulate the high ozone episode in the YRD in 2010. The CMAQ model domain is based on a Lambert Conformal map projection, using a one-way nested mode with grid resolutions of 81 km (covering all China, Japan, Korea, parts of India and Southeast Asia); 27 km (covering Eastern China) and 9 km (covering major city-clusters including Shandong province, the YRD and the Pearl River Delta (PRD)). The large domain is centered at (118° E, 32° N). The model domain is shown in Fig. 1. The MM5 domain is larger than the CMAQ domain, with three grids more than the CMAQ domain on each boundary. The time period chosen for simulation is 1–31 August 2010, when the YRD experienced high ozone concentrations. The initial conditions of CMAQ are prepared by running the model three days ahead of each start date with clean initial conditions (IC). The boundary condition (BC) used for the largest domain of CMAQ is clean air, while the BCs for the nested domains are extracted from the CMAQ Chemical Transport Model (CCTM) concentration files of the larger domain. Both the MM5 and CMAQ employ 14 vertical layers of varying thickness with denser layers in the lower atmosphere to better resolve the mixing height.

The driving meteorological inputs for CMAQ are provided by MM5, and the meteorology-chemistry interface processor (MCIP) is used to transfer MM5 output into gridded meteorological field data as the input to CMAQ. The inputs for MM5 are NCEP FNL (Final) Operational Global Analysis data, which are available on 1.0° × 1.0° grids continuously for every 6 h (http://dss.ucar.edu/datasets/ds083.2/). The Carbon Bond 05 chemical mechanism (CB05) is used in the CMAQ model (Sarwar, 2008).

ACPD
12, 15049–15082, 2012

Geographic Information System (GIS) technology is applied in gridding the YRD regional emission inventory to the model domain. The newly calculated emissions for the YRD in 2007 (Huang et al., 2011) are updated to the year 2010 based on energy consumption and are then inserted into the regional East Asian emission inventory provided by INTEX-B (Streets et al., 2003a,b; Fu et al., 2008; Zhang et al., 2009). For biogenic VOC emissions, this study uses the natural VOC emission inventory of the GEIA Global Emissions Inventory Activity 1990 (http://geiacenter.org).

2.2 Model evaluation protocol

Predicted meteorological parameters including wind speed, wind direction, temperature and humidity are compared with the hourly observational data obtained during August 2010. Performance statistics of MM5 are calculated with application of the Metstat statistical analysis package (Emery et al., 2001).

The simulation of O_3 formation during 5–31 August is evaluated against observations made at the supersite in Shanghai Academy of Environmental Sciences (SAES). The measurements are collected simultaneously at the surface site. The levels of O_3 and NO_x were measured by Ecotech commercial instruments EC9811 and EC9841A, respectively.

The model performance is judged by statistical measures, including the normalized mean bias (NMB), index of agreement (I), correlation coefficient (R), and factor of two.

ACPD
12, 15049–15082, 2012

The NMB, I and Factor of two are calculated by Eqs. (1)–(3):

$$\mathrm{NMB} = \frac{\sum_{i=1}^{N}(p_i - o_i)}{\sum_{i=1}^{N} o_i} \cdot 100\% \quad (1)$$

$$I = 1 - \frac{\sum_{i=1}^{N}(p_i - o_i)^2}{\sum_{i=1}^{N}\left(\left|p_i - \overline{o}\right| + \left|o_i - \overline{o}\right|\right)^2} \quad (2)$$

$$R = \frac{N_{[1/2,2]}}{N_t} \quad (3)$$

where p_i represents the predicted data and o_i represents the observational data. N means the number of data pairs. $\overline{o}$ denotes the average observed concentration and a value of 1 indicates perfect agreement between predicted and observed values. R is the percentage of the ratios between 0.5 and 2; $N_{[1/2,2]}$ is the number of the ratios between 0.5 and 2; and N_t is the total number of comparison pairs. The larger the R value, the better the model performs. R = 100 % means the model performance is perfect.

2.3 Integrated process rate analysis

Quantifying the contributions of individual processes to model predictions provides a fundamental explanation and shows the relative importance of each process. IPR analysis deals with the effects of all the physical processes and the net effect of chemistry on model predictions. The IPR analysis calculates hourly contributions of horizontal advection and diffusion, vertical advection and diffusion, dry deposition, gas-phase chemistry, clouds process and aqueous chemistry, etc. The IPR method has

ACPD
12, 15049–15082, 2012

been widely applied to regional photochemical pollution studies (Xu and Zhang, 2006; Xu et al., 2008; Goncalves et al., 2009; Wang et al., 2009; Zhang et al., 2009a,b).

2.3.1 Episode Selected for process analysis

The 16–17 August 2010, is a typical summertime situation, with average surface temperature of 30.5 °C, maximum temperature of 36.7 °C, occurring at 12:00 LST on 16 August. The average relative humidity was 63.5 %, and the wind speed was lower than 1 m s^{-1} during the period. The observed maximum surface hourly O_3 concentration was 86 ppb, which is very rare in an urban site of Shanghai region. In this paper, 16–17 August is used for the IPR analysis because the high ozone episode was observed at the SAES observational site.

For the IPR analysis, we first assess the roles of various atmospheric processes in O_3 formation at the supersite located in Shanghai Academy of Environmental Sciences, Xuhui District, which represents a typical site in urban Shanghai, and in Jinshan District, a chemical industrial site with high VOC emissions, which reflects the influences of pollutants transported from upwind areas and local precursor emissions. We then investigate the influences of different processes on the formation and evolution of regional O_3 pollution over the YRD region as a whole. The sites we selected include two provincial capital cities, Nanjing and Hangzhou. Nanjing is located in Jiangsu province, northwest of Shanghai, and Hangzhou is located in Zhejiang province, southwest of Shanghai. Locations of the sites selected to do O_3 process analysis in this study are shown in Fig. 2.

3 Results and discussion

3.1 Evaluation of model performance

Table 1 shows comparisons between observed and modeled meteorological parameters including surface temperature, wind speed, wind direction and relative humidity

ACPD
12, 15049–15082, 2012

during the period of 5–31 August 2010 at four surface stations in Shanghai, namely Baoshan (BS), Jinshan (JS), Nanhui (NH) and Qingpu (QP), shown in Fig. 2. Figure 3 gives average data for the four meteorology monitoring sites. The average bias of wind speed, wind direction, temperature and humidity are 0.65, 2.5, 0.13 and −0.81, respectively. Figure 3 shows the daily comparisons of the meteorological parameters, which indicates that MM5 can reflect the variation trends of the major meteorological conditions. The selected parameters adopted in MM5 can be used in the pollutant concentration simulation.

Figure 4 shows the comparisons between model results and observational data for O_3, NO_2, NO_x and NO_y hourly concentrations at Shanghai during 5–31 August 2010. Results show that CMAQ can reproduce the variation trends of the O_3, with a correlation coefficient of 0.78, NMB of 30.2 %, NME of 55.8 %, and *I* of 0.91, comparable to the performance of other CMAQ applications (Goncalves et al., 2009; Shen et al., 2011). The model also reproduces the daily change of O_3 concentration. With increase of solar radiation early in the day, the O_3 concentration rises; while in the afternoon, with decrease of radiation, the O_3 concentration gradually declines. Comparisons of precursor concentrations including NO_2, NO_x and NO_y at the monitoring site further demonstrate that the O_3 formation is captured reasonably well over the domain and throughout the period. The index of agreement for NO_2, NO_x and NO_y are 0.91, 0.63 and 0.64, respectively, as shown in Table 2.

3.2 Process analysis of ozone formation

3.2.1 Urban area of Shanghai

The contributions of different atmospheric processes to the evolution of O_3 in the urban Shanghai area (Xuhui) from 16 to 17 August, 2010 at different layers are shown in Fig. 5. As shown in the figure, in the first layer (0–40 m) of the urban Shanghai area, the major contributors to high O_3 concentrations in daytime include vertical diffusion (VDIF), vertical advection (ZADV) and horizontal advection (HADV), while gas-phase

ACPD
12, 15049–15082, 2012

chemistry (CHEM) exhibited a significant consumption of O_3 during most times of the day except 10:00–16:00 LST, due to the high emissions of NO_x from vehicle exhausts. During the simulation period, the average positive contributions of vertical diffusion and horizontal transport are 24.7 ppb h^{-1}, 3.6 ppb h^{-1}, accounting for 27.6 % and 6.6 %, respectively. Photochemistry, dry deposition (DDEP) and vertical advective transport are three major sinks of O_3. The average contributions of CHEM, DDEP and ZADV to O_3 change are −21.9, −4.3 and −2.1 ppb h^{-1}, accounting for −25.3 %, −5.0 % and −3.7 %, respectively.

During the buildup of daytime maximum O_3 from 10:00 to 12:00 LST on both 16 and 17 August, gas-phase chemistry also plays an important role in the formation of high O_3 concentrations. The maximum O_3 concentration approached 75.3 ppb and 86.2 ppb at 12:00 and 11:00 LST on 16 and 17 August, respectively. In the early morning hours of the episode, O_3 levels produced by local photochemistry were rarely zero. After 10:00 LST, the photochemistry contribution to O_3 formation became obvious, with the highest positive concentration of 27 ppb h^{-1} and 21.7 ppb h^{-1} to the hourly O_3 concentration, accounting for 58 % and 20 % on 16 and 17 August, respectively. The O_3 maximum concentrations during the 16–17 August occur at 11:00 LST on 17 August, 2010. At this time, the horizontal advective transport into the area constitutes the major positive contribution to net O_3, with the ozone formation rate of 27.4 ppb h^{-1}, accounting for 25.6 % of net surface O_3 production; photochemistry is the second largest contributor, with the ozone formation rate of 21.7 ppb h^{-1} and 20.3 % of positive contribution. There is also a significant vertical advective transport from the upper layer, with 10.7 ppb h^{-1}. Later on, until 17:00 LST, the horizontal advective flows remove O_3 from this area, with −56.5 ppb h^{-1} on average, due to the transport of the pollution plume.

During the IPR analysis period, the O_3 increase by both horizontal transport and photochemistry was stronger at 300–1500 m height than in the surface layer, making a strong vertical O_3 transport from upper levels to the surface layer. This indicates that the strong vertical O_3 import at surface layer is initiated by the urban plume arrival. On 17 August, high O_3 input by transport occurred later in the afternoon, arising from

ACPD
12, 15049–15082, 2012

well-developed photochemistry in the urban plume, thereby further enhancing the O_3 concentrations in urban Shanghai area and leading to another high O_3 episode, approaching 86 ppb.

3.2.2 Suburban and industrial area of Shanghai

The Jinshan District (JS) is located in the southwest of urban Shanghai area. It belongs to an oil and chemistry industrial region. Lots of petrochemical enterprises, including Shanghai Jinshan Photochemical Company are located in this region. Compared to urban Shanghai area with lots of NO_x emissions from motor vehicles, the emissions of volatile organic compounds (VOCs) are much more significant. As shown in Fig. 6, The major processes controlling the surface ozone production in the JS site during the daytime on both days include photochemical reaction, vertical diffusion and horizontal advective transport, while dry deposition and vertical advective transport are the most significant sink of O_3 concentrations. During the simulation period, the average positive contributions of vertical diffusion and horizontal transport are 25.8 ppb h^{-1}, 10.3 ppb h^{-1}, accounting for 25.9 % and 11.3 % of net O_3 change, respectively. The average O_3 production rate contributed by dry deposition and vertical advective transport are −24.1, and −11.9 ppb h^{-1}, accounting for −20.5 % and −11.2 % of net O_3 change, respectively.

The O_3 production rates from chemistry during 10:00–14:00 LST on 16–17 August, 2010 are between 8.2–45.4 ppb h^{-1}. The maximum ozone production rates from photochemical reaction were 45.4 and 23.3 ppb h^{-1}, occurring at 12:00 on 16 August and 14:00 on 17 August, with the contribution of 20.4 % and 12.9 %, respectively. The processes contributions to net surface O_3 concentrations assessed in JS site during this period indicates that net transport (ZADV + HADV + HDIF + VDIF) accounts for 26.3 % and chemical reaction for −11.1 %.

ACPD
12, 15049–15082, 2012

The daily change of O_3 concentrations are most significant in surface layers, however, the diurnal change becomes less with vertical height. At the 900–1400 m height, the ozone concentrations retain around 50 ppb.

3.2.3 Nanjing, the capital city of Jiangsu province

The surface O_3 concentrations in Nanjing, the capital city of Jiangsu province, have been modeled and the IPR analysis was applied into the process contribution calculation. As shown in Fig. 7, The major processes controlling the surface ozone production at the Nanjing site during the daytime on both days include vertical diffusion and horizontal transport, while photochemical reaction, vertical advective transport and dry deposition are the most significant sinks of O_3. During the simulation period, the average O_3 production rates contributed by vertical diffusion and horizontal transport are 25.3 ppb h^{-1}, 15.3 ppb h^{-1}, accounting for 25.8 % and 18.5 % of net O_3 change, respectively. The average contributions of photochemistry, vertical advective transport and dry deposition to O_3 change are −30.6, −6.2 and −3.7 ppb h^{-1}, accounting for −31.8 %, −7.3 % and −4.7 %, respectively. The maximum surface O_3 concentration was 88.7 ppb, occurring at 12:00 LST on 16 August, 2010. At this time, the O_3 production rate from chemistry is 46.7 ppb h^{-1}, accounting for 59.4 % of the net O_3 concentration change. The processes contributions to net surface O_3 concentrations assessed at the Nanjing site during this period indicate that net transport accounts for 9 % and chemical reaction for −32 %.

However, if we look at the O_3 concentration change in the height of 350–500 m and 500–900 m, we can see that during the time period of 10:00–15:00 LST, photochemistry plays the most important role in net O_3 production. The highest positive contributions from gas-phase chemistry to net O_3 production in the height of 350–500 m and 500–900 m reached 87.3 % and 68.6 %, respectively, and making a strong vertical O_3 transportation from the upper level to the surface layer.

ACPD
12, 15049–15082, 2012

3.2.4 Hangzhou, the capital city of Zhejiang province

Although during 16–17 August 2010, Shanghai and Nanjing experienced high O_3 concentrations, a similar situation did not occur in Hangzhou. Modeling results show that the highest O_3 concentration in the cell of Hangzhou during this period was only 59.0 ppb, occurring at 15:00 LST on 17 August, 2010. The O_3 concentrations in layer 7 (350–500 m) and 8 (500–900 m) are generally higher than the ground layer, which is around 50 ppb during the whole simulation period. As shown in Fig. 8, The major processes controlling the surface ozone production in the Hangzhou site during the daytime on both days include vertical diffusion, while dry deposition are the most significant sink of O_3 concentrations. During the simulation period, the average positive contribution of vertical diffusion is 21.4 ppb h^{-1}, accounting for 28.9 %. During the buildup of daytime maximum O_3 from 10:00 to 14:00 LST on both 16 and 17 August, gas-phase chemistry also plays an important role in the formation of net surface O_3 production. The average positive contributions to O_3 are 12.6 and 7.0 ppb h^{-1}, accounting for 10.7 % and 6.2 % during this time period on 16 and 17 August, 2010, respectively. The process contributions to net surface O_3 concentrations assessed in Hangzhou site during this period indicates that net transport accounts for 9 % and chemical reaction for −9 %.

3.3 Regional ozone transport

Figure 9 shows the time series of meteorological conditions and O_3 and NO_x mass concentrations observed at the site of SAES during the high O_3 pollution episodes on 16–17 August, 2010. During the pollution episode, the NO_x, O_3 and O_x ($NO_2 + O_3$) continued to increase. Daily average concentrations of NO_2 and O_x were 23.4 ppb and 57.5 ppb on 16 August, and increased to 35.0 ppb and 66.5 ppb on 17 August 2010, respectively. The maximum hourly concentration of O_3 increased from 75.1 ppb on 16 August to 86.5 ppb on 17 August 2010. During the period, the air temperature was around 30 °C, with the highest temperature of 36.7 °C at 12:00 on 16 August and

ACPD
12, 15049–15082, 2012

34.7 °C at 12:00 on 17 August 2010. The highest solar radiation levels were 786 and 571 $W m^{-2}$ on 16 and 17 August, respectively. Under the high atmospheric oxidation conditions, the NO was rapidly oxidized to NO_2, which is later converted to O_3 by photolytic destruction.

The O_3 concentrations in most urban cities during the night time (0:00–6:00) are very low, because the high NO emissions in the urban area gradually titrate ozone, which causes the ozone concentration to decrease. However, the NO emissions in the rural area are much lower, which preserves the high ozone concentration.

The O_3 concentration in the Yangtze River Delta started to accumulate from 8:00 on 16 August, 2010. As shown in Fig. 10, from 8:00 on 16 August, the O_3 concentrations started to rise in the cities of Suzhou, Hangzhou and Ningbo. Under the southwest wind direction, this ozone started to diffuse to Shanghai and the surrounding area. From 10:00 on 16 August, the O_3 production from photochemistry in major cities like Hangzhou, Ningbo, Shanghai and Suzhou is high. The maximum ozone production rates from photochemical reaction reached 45.4 ppb h^{-1}, occurring at 12:00 on 16 August, with the contribution of 20.4 % to the total O_3. Later on, the O_3 is transported to the ocean under the westerly wind, and then flows back to North Shanghai and South Jiangsu area due to the northeast wind off the sea. After sunset, the O_3 concentrations started to decrease.

On the next day, the O_3 was produced from chemical reactions in the cities of Shanghai, Hangzhou, Suzhou, Wuxi and Nanjing from 10:00 on 17 August 2010. The O_3 transported during 10:00–15:00 is mainly surrounding the Shanghai area, since the wind speed is relatively low, as shown from both Figs. 9 and 10. Later on, it spreads to the northwest part of the region, including Nanjing, under the easterly wind. On this day, although the solar radiation and the highest air temperature are both lower than the previous day, the highest O_3 concentration occurs in Shanghai. This is because the wind speed is low, and the horizontal transport from the surrounding area is greater than the previous day, while diffusion to the other regions is low.

ACPD
12, 15049–15082, 2012

4 Conclusions

The Community Multi-scale Air Quality modeling system (CMAQ) was applied to investigate the high O_3 pollution episodes over the YRD region during August, 2010. The modeling results agree well with the observational data, and the model reproduced the concentration levels and variations. Model performance evaluation shows that the model is suitable for the simulation and prediction of photochemical pollution.

The Integrated Process Rate implemented in the CMAQ model was applied to obtain quantitative information about atmospheric processes affecting the ozone concentration in typical cities located in the Yangtze River Delta area, including Shanghai, Nanjing and Hangzhou. A representative summertime photochemical pollution episode (16–17 August, 2010) was selected. Applying the Integrated Process Rate tool to the first vertical layer simulated provides information about the surface concentration of pollutants estimated by the model. In order to perform a deeper study of the contributions of the main atmospheric processes leading to the levels of these pollutants, the vertical ozone production in layer 1 (0–40 m), layer 7 (350–500 m), layer 8 (500–900 m) and layer 10 (1400–2000 m) have been examined.

Process analysis indicates that the maximum concentration of photochemical pollutants occur due to transport phenomena, including vertical transport and horizontal transport. The gas-phase chemistry producing O_3 mainly occurs in the height of 300–1500 m, making a strong vertical O_3 transportation from upper level to the surface layer. In the downwind area, the high surface O_3 levels are not produced in situ, but come from horizontally advected flows during the morning and gas-phase chemical contributions occurring aloft. The urban Shanghai domain behavior slightly differs: the horizontal advection is also the main contributor to O_3 surface concentrations, but the chemical formation takes place in the whole vertical column below the PBL.

The gas-phase chemistry is an important sink for O_3 in the lowest layer, coupled with vertical advection flows and dry deposition. The horizontal diffusive processes contributions to net O3 concentrations under the PBL are relatively low, which is negligible

ACPD
12, 15049–15082, 2012

compared to other atmospheric processes. The diffusive processes contributions to net O_3 concentrations under the PBL are relatively low, and in particular the horizontal diffusion is negligible compared to other atmospheric processes. Vertical diffusion compensates the loss of O_3 in surface layers due to NO titration, contributing positively to net O_3 concentrations in urban areas. The O_3 peaks at surface level are higher in the suburban industrial region (Jinshan), mainly due to the much simpler transport pattern compared to the downtown region, together with the more significant photochemistry. The cloud processes, wet deposition and heterogeneous chemistry contributions are negligible during the whole episode, characterized by high solar radiation and no precipitation or cloudiness.

As shown by the modeling results, the O_3 pollution characteristics among the different cities in the YRD region have both similarities and differences. During the buildup period (usually from 8:00 in the morning after sunrise), the O_3 starts to appear in the city regions like Shanghai, Hangzhou, Ningbo and Nanjing and is then transported to the surrounding areas under the prevailing wind conditions. On both days, the O_3 production from photochemical reaction in Shanghai and the surrounding area are most significant, due to the high emission intensity in the large city; this ozone is then transported out to sea by the westerly wind flow, and later diffuses to rural areas like Chongming island, Wuxi and even to Nanjing. The O_3 concentrations start to decrease in the cities after sunset, due to titration of the NO emissions, but ozone can still be transported and maintain a significant concentration in rural areas and even regions outside the YRD region, where the NO emissions are very small.

This work explores the possibilities of applying process analysis to high ozone pollution episodes, proving that it is useful not only to better evaluate the simulation results, but also to perform more accurate source apportionment of pollutants over a region. Results show that to control O_3 pollution, the measures should be taken locally and regionally as well.

Acknowledgements. This study was supported by the National Non-profit Scientific Research Program for Environmental Protection via grants No. 201009001 and the Science and

ACPD
12, 15049–15082, 2012

Technology Commission of Shanghai Municipality Fund Project via grants No. 11231200500, and No. 10231203802. The authors appreciate the suggestions made by the reviewers that helped greatly to improve this paper.

References

An, X., Zhu, T., Wang, Z., Li, C., and Wang, Y.: A modeling analysis of a heavy air pollution episode occurred in Beijing, Atmos. Chem. Phys., 7, 3103–3114, doi:10.5194/acp-7-3103-2007, 2007.

Byun, D. W., Ching, J. K. S., Novak, J., and Young, J.: Development and Implementation of the EPA's Models-3 Initial Operating Version: Community Multi-Scale Air Quality (CMAQ) Model, Plenum Publishing Corp., New York, USA, 1998.

Byun, D. W. and Ching, J. K. S.: Science algorithms of the EPA Models-3 Community Multi-scale Air Quality (CMAQ) modeling system, US Environmental Protection Agency Report EPA/600/R-99/030, Research Triangle Park, NC, 1999.

Chan, C. K. and Yao, X.: Air pollution in mega cities in China, Atmos. Environ., 1, 1–42, 2008.

Chou, C. C.-K., Tsai, C.-Y., Chang, C.-C., Lin, P.-H., Liu, S. C., and Zhu, T.: Photochemical production of ozone in Beijing during the 2008 Olympic Games, Atmos. Chem. Phys., 11, 9825–9837, doi:10.5194/acp-11-9825-2011, 2011.

Dennis, R. L., Byun, D. W., Novak J. H., Galluppi K. J., Coats, C. J., and Vouk, M. A.: The next generation of integrated air quality modeling: EPA's Models-3, Atmos. Environ., 30, 1925–1938, 1996.

Emery, C. A., Tai, E., and Yarwood, G.: Enhanced meteorological modeling and performance evaluation for two Texas ozone episodes, Project Report prepared for the Texas Natural Resource Conservation Commissions, ENVIRON International Corporation, Novato, CA, 2001.

Fu, J. S., Jang, C. J., Streets, D. G., Li, Z., Kwok, R., Park, R., and Han, Z.: MICS-Asia II: modeling gaseous pollutants and evaluating an advanced modeling system over East Asia, Atmos. Environ., 42, 3571–3583, 2008.

Gonçalves, M., Jiménez-Guerrero, P., and Baldasano, J. M.: Contribution of atmospheric processes affecting the dynamics of air pollution in South-Western Europe during a typical summertime photochemical episode, Atmos. Chem. Phys., 9, 849–864, doi:10.5194/acp-9-849-2009, 2009.

ACPD

12, 15049–15082, 2012

Huang, C., Chen, C. H., Li, L., Cheng, Z., Wang, H. L., Huang, H. Y., Streets, D. G., Wang, Y. J., Zhang, G. F., and Chen, Y. R.: Emission inventory of anthropogenic air pollutants and VOC species in the Yangtze River Delta region, China, Atmos. Chem. Phys., 11, 4105–4120, doi:10.5194/acp-11-4105-2011, 2011.

Li, L., Chen, C. H., Fu, J. S., Huang, C., Streets, D. G., Huang, H. Y., Zhang, G. F., Wang, Y. J., Jang, C. J., Wang, H. L., Chen, Y. R., and Fu, J. M.: Air quality and emissions in the Yangtze River Delta, China, Atmos. Chem. Phys., 11, 1621–1639, doi:10.5194/acp-11-1621-2011, 2011.

Ran, L., Zhao, C., Geng, F., Tie, X., Tang, X., Peng, L., Zhou, G., Yu, Q., Xu, J., and Guenther, A.: Ozone photochemical production in urban Shanghai, China: analysis based on ground level observations, J. Geophys. Res., 114, D15301, doi:10.1029/2008JD010752, 2009.

Sarwar, G., Luecken, D., Yarwood, G., Whitten, G. Z., and Carter, W. P. L.: Impact of an updated carbon bond mechanism on predictions from the CMAQ Modeling System: preliminary assessment, J. Appl. Meteor. Climatol., 47, 3–14, doi:10.1175/2007JAMC1393.1, 2008.

Seinfeld, J. H. and Pandis, S. N.: Atmospheric Chemistry and Physics: from Air Pollution to Climate Change, 2nd edn., John Wiley & Sons, New York, 2006.

Shao, M., Zhang, Y. H., Zeng, L. M., Tang, X. Y., Zhang, J., Zhong, L. J., and Wang, B. G.: Ground-level ozone in the Pearl River Delta and the roles of VOC and NO_x in its production, J. Environ. Manage., 90, 512–518, 2009.

Shen, J., Wang, X. S., Li, J. F., Li, Y. P., and Zhang Y. H.: Evaluation and intercomparison of ozone simulations by Models-3/CMAQ and CAMx over the Pearl River Delta, Science China (Chemistry), 54, 1789–1800, 2011.

Streets, D. G., Bond, T. C., Carmichael, G. R., Fernandes, S. D., Fu, Q., He, D., Klimont, Z., Nelson, S. M., Tsai, N. Y., Wang, M. Q., Woo, J. H., and Yarber, K. F.: An inventory of gaseous and primary aerosol emissions in Asia in the year 2000, J. Geophys. Res., 108, 8809, doi:10.1029/2002JD003093, 2003a.

Streets, D. G., Yarber, K. F., Woo, J.-H., and Carmichael, G. R.: Biomass burning in Asia: annual and seasonal estimates and atmospheric emissions, Global Biogeochem. Cy., 17, 1099, doi:10.1029/2003GB002040, 2003b.

Tang, G., Li, X., Wang, Y., Xin, J., and Ren, X.: Surface ozone trend details and interpretations in Beijing, 2001–2006, Atmos. Chem. Phys., 9, 8813–8823, doi:10.5194/acp-9-8813-2009, 2009.

ACPD
12, 15049–15082, 2012

Wang, H., Kiang, C. S., Tang, X., Zhou, X., and Chameides, W.: Surface ozone: a likely threat to crops in Yangtze delta of China, Atmos. Environ., 39, 3843–3850, 2005.
Wang, K., Zhang, Y., Jang, C., Phillips, S., and Wang, B. Y.: Modeling intercontinental air pollution transport over the trans-Pacific region in 2001 using the Community Multiscale Air Quality modeling system, J. Geophys. Res., 114, D04307, doi:10.1029/2008JD010807, 2009.
Wang, T., Ding, A. J., Gao, J., and Wu, W. S.: Strong ozone production in urban plumes from Beijing, China, Geophys. Res. Lett., 33, L21806, doi:10.1029/2006GL027689, 2006.
Wang, T., Nie, W., Gao, J., Xue, L. K., Gao, X. M., Wang, X. F., Qiu, J., Poon, C. N., Meinardi, S., Blake, D., Wang, S. L., Ding, A. J., Chai, F. H., Zhang, Q. Z., and Wang, W. X.: Air quality during the 2008 Beijing Olympics: secondary pollutants and regional impact, Atmos. Chem. Phys., 10, 7603–7615, doi:10.5194/acp-10-7603-2010, 2010.
Wang, X., Zhang, Y., Hu, Y., Zhou, W., Lu, K., Zhong, L., Zeng, L., Shao, M., Hu, M., and Russell, A. G.: Process analysis and sensitivity study of regional ozone formation over the Pearl River Delta, China, during the PRIDE-PRD2004 campaign using the Community Multiscale Air Quality modeling system, Atmos. Chem. Phys., 10, 4423–4437, doi:10.5194/acp-10-4423-2010, 2010.
Wang, Y., Hao, J., McElroy, M. B., Munger, J. W., Ma, H., Chen, D., and Nielsen, C. P.: Ozone air quality during the 2008 Beijing Olympics: effectiveness of emission restrictions, Atmos. Chem. Phys., 9, 5237–5251, doi:10.5194/acp-9-5237-2009, 2009.
Xu, J. and Zhang, Y. H.: Process analysis of O_3 formation in summer at Beijing, Acta Sci. Circum., 26, 973–980, 2006.
Xu, J., Zhang, Y. H., and Wang, W.: Numerical study on the impacts of heterogeneous reactions on ozone formation in the Beijing urban area, Adv. Atmos. Sci., 23, 605–614, 2006.
Xu, J., Zhang, Y., Fu, J. S., and Wang, W.: Process analysis of typical ozone episode in summer over Beijing area, Sci. Total Environ., 399, 147–157, 2008.
Xu, X., Lin, W., Wang, T., Yan, P., Tang, J., Meng, Z., and Wang, Y.: Long-term trend of surface ozone at a regional background station in eastern China 1991–2006: enhanced variability, Atmos. Chem. Phys., 8, 2595–2607, doi:10.5194/acp-8-2595-2008, 2008.
Xu, X. B., Lin, W. L., Wang, T., Meng, Z. Y., and Wang, Y.: Long-term trend of tropospheric ozone over the Yangtze Delta Region of China, Adv. Clim. Change Res., 3, 60–65, 2007.
Zhang, Q., Streets, D. G., Carmichael, G. R., He, K. B., Huo, H., Kannari, A., Klimont, Z., Park, I. S., Reddy, S., Fu, J. S., Chen, D., Duan, L., Lei, Y., Wang, L. T., and Yao, Z. L.: Asian

ACPD
12, 15049–15082, 2012

emissions in 2006 for the NASA INTEX-B mission, Atmos. Chem. Phys., 9, 5131–5153, doi:10.5194/acp-9-5131-2009, 2009.

Zhang, Y., Vijayaraghavan, K., Wen, X. Y., Snell, H. E., and Jacobson, M. Z.: Probing into regional ozone and particulate matter pollution in the United States: 1. a 1 year CMAQ simulation and evaluation using surface and satellite data, J. Geophys. Res., 114, D22304, doi:10.1029/2009JD011898, 2009a.

Zhang, Y., Vijayaraghavan, K., Wen, X. Y., Snell, H. E., and Jacobson, M. Z.: Probing into regional O_3 and particulate matter pollution in the United States: 2. An examination of formation mechanisms through a process analysis technique and sensitivity study, J. Geophys. Res., 114, D22305, doi:10.1029/2009JD011900, 2009b.

Zhang, Y. H., Su, H., Zhong, L. J., Cheng, Y. F., Zeng, L. M., Wang, X. S., Xiang, Y. R., Wang, J. L., Gao, D. F., Shao, M., Fan, S. J., and Liu, S. C.: Regional ozone pollution and observation-based approach for analyzing ozone-precursor relationship during the PRIDE-PRD2004 campaign, Atmos. Environ., 42, 6203–6218, 2008.

Zhao, C. S., Peng, L., Sun, A. D., Qin, Y., Liu, H. L., Li, W. L., and Zhou, X. J.: Numerical modeling of tropospheric ozone over Yangtze Delta region, Acta Sci. Circum., 24, 525–533, 2004.

ACPD

12, 15049–15082, 2012

Table 1. Statistical results between MM5 model and observation data at surface stations in Shanghai.

		BS	JS	NH	QP	Average
Wind Speed	RMSE ($m s^{-1}$)	1.76	1.43	1.13	1.24	1.39
	Bias ($m s^{-1}$)	0.94	0.57	0.43	0.65	0.65
	IOA	0.4	0.44	0.57	0.51	0.48
Wind Direction	Gross Error (°)	38.02	30.88	29.43	39.79	34.53
	Bias (°)	3.21	4.55	−2.83	5.05	2.50
Temperature	Gross Error (K)	0.82	1.18	1.55	1.21	1.19
	Bias (K)	−0.91	−0.71	1.36	0.77	0.13
	IOA	0.76	0.81	0.83	0.9	0.83
Relative Humidity	Gross Error ($g kg^{-1}$)	1.15	1.18	1.85	2.95	1.78
	Bias ($g kg^{-1}$)	−0.14	−0.81	−1.67	−0.6	−0.81
	IOA	0.4	0.49	0.36	0.38	0.41

ACPD
12, 15049–15082, 2012

Table 2. Statistical results between CMAQ model and observation data during 5–31 August 2010.

Species	Number of data pairs	Correlation coefficient	NMB (%)	NME (%)	/
O_3	672	0.78	30.22 %	55.83 %	0.91
NO_2	672	0.53	13.78 %	48.41 %	0.91
NO_x	669	0.42	−2.67 %	50.51 %	0.63
NO_y	669	0.45	−5.10 %	48.55 %	0.64

ACPD
12, 15049–15082, 2012

Table 3. Comparisons between the modeled hourly, max and min data against observations of surface O_3, NO_2, NO_x and NO_y during 5–31 August 2010.

	O_3		NO_2		NO_x		NO_y	
	Observation	Model	Observation	Model	Observation	Model	Observation	Model
Hourly	42.92	55.90	38.56	21.97	26.82	25.98	28.78	27.19
Max	87.00	123.46	79.00	83.31	172.70	96.62	196.39	98.41
Min	3.20	0.00	0.00	3.93	6.70	4.54	5.43	1.27

ACPD
12, 15049–15082, 2012

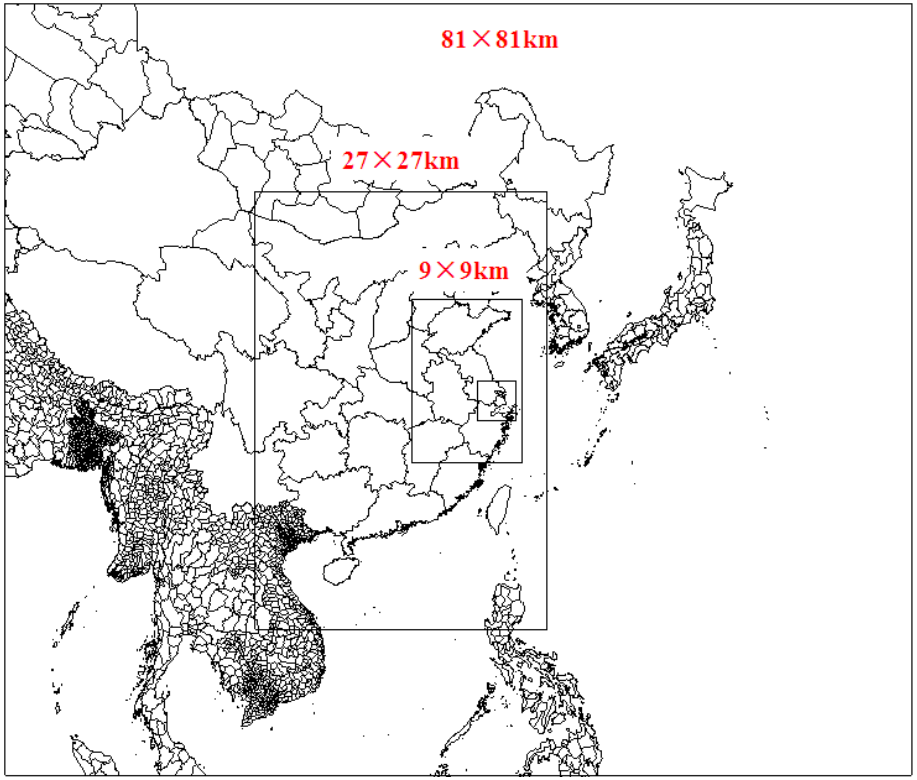

Fig. 1. One-way nested CMAQ model domain.

ACPD
12, 15049–15082, 2012

Fig. 2. Locations selected to do O_3 process analysis (left) and meteorological stations to do MM5 model evaluation (right) in the YRD.

ACPD
12, 15049–15082, 2012

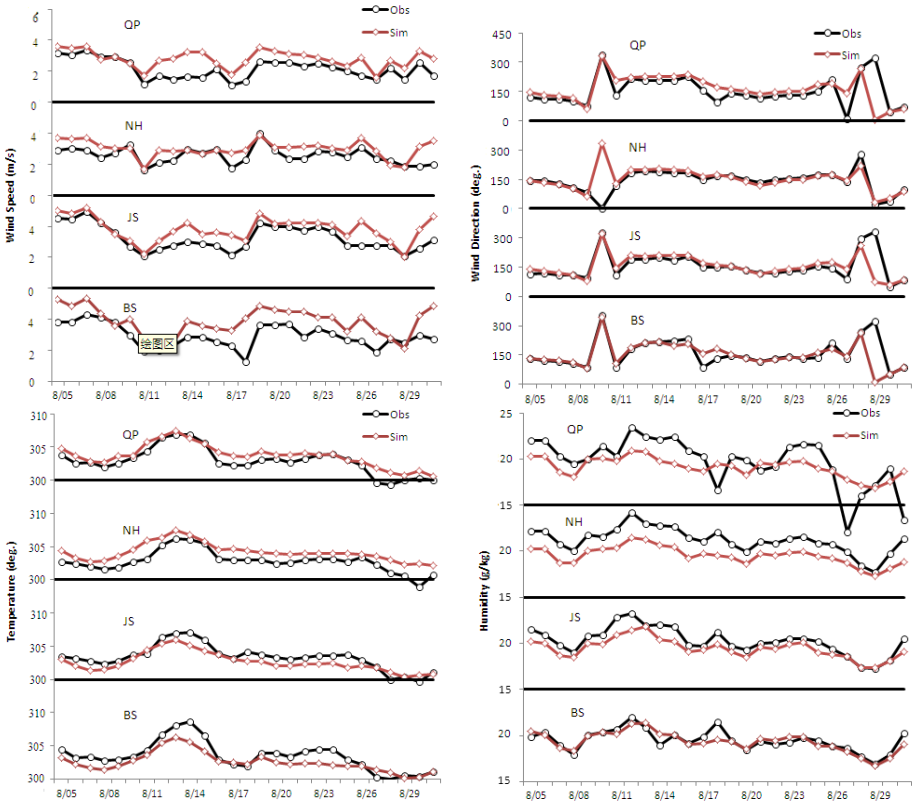

Fig. 3. Time series of simulated surface wind speed, wind direction, temperature and relative humidity compared with observations at four monitoring sites during 5–31 August 2010.

ACPD
12, 15049–15082, 2012

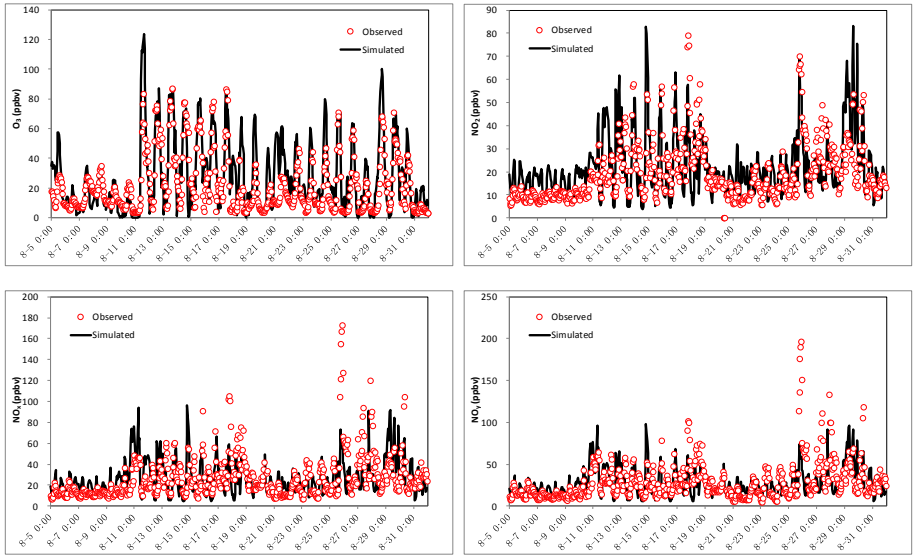

Fig. 4. Time series of simulated surface O_3, NO_2, NO_x and NO_y against that observed at SAES monitoring site during 5–31 August 2010.

ACPD
12, 15049–15082, 2012

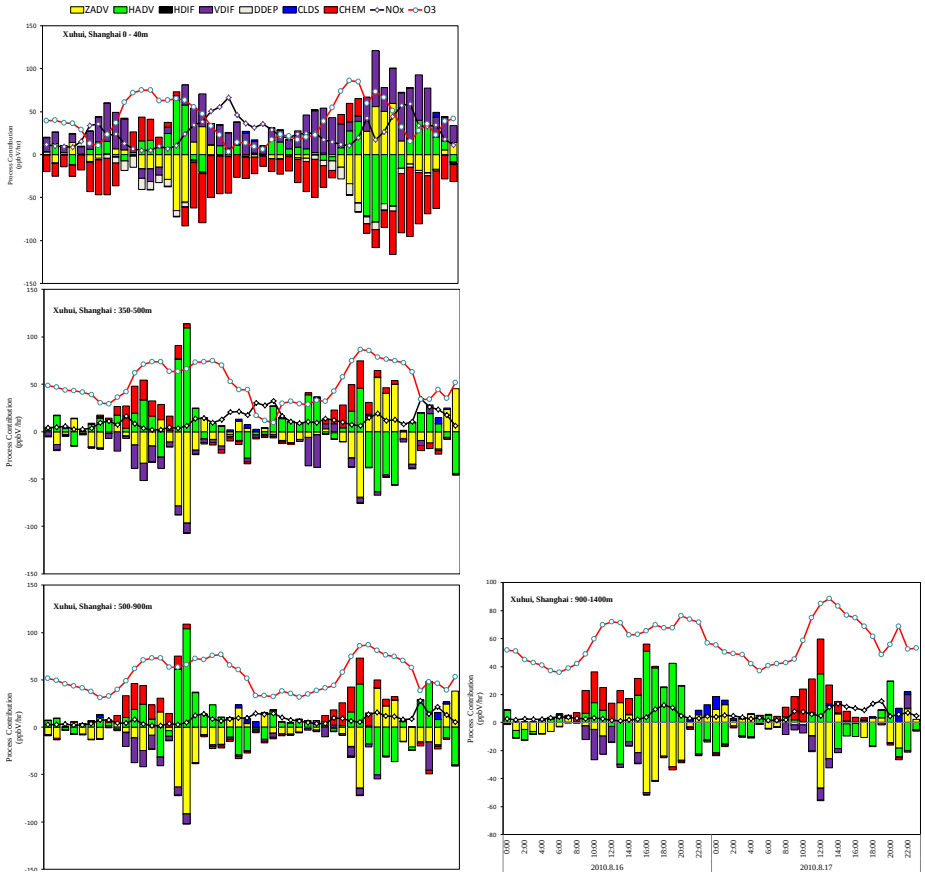

Fig. 5. Atmospheric processes contribution to net O_3 density at Xuhui site during 16–17 August 2010.

ACPD
12, 15049–15082, 2012

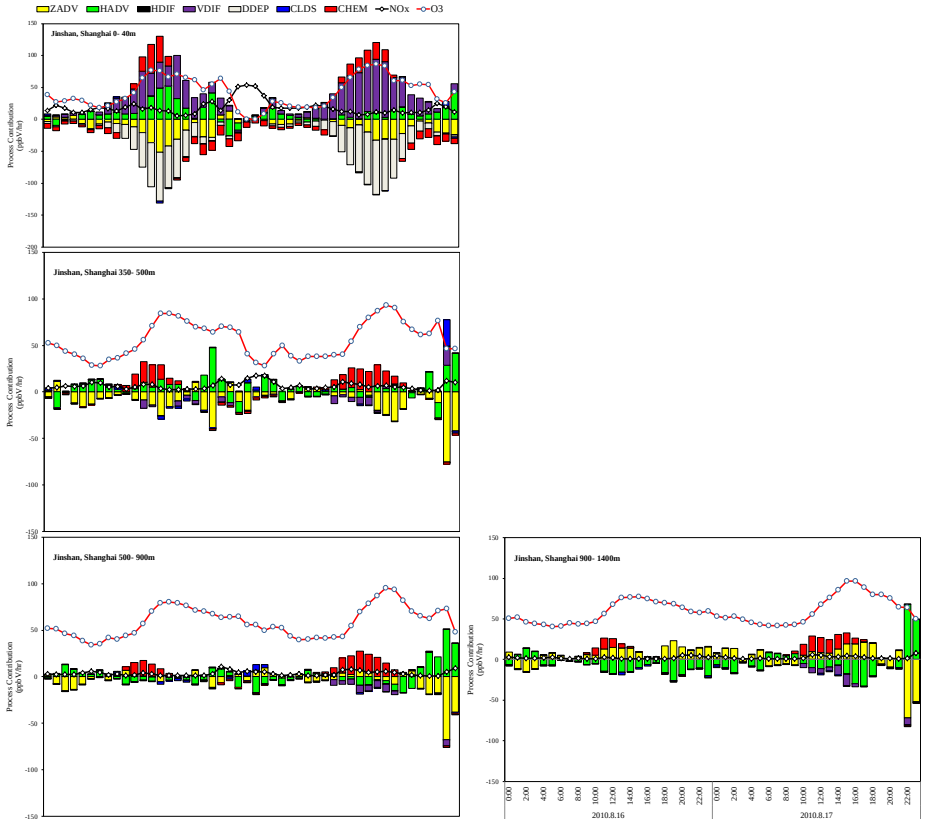

Fig. 6. Atmospheric processes contribution to net O_3 density at Jinshan site during 16–17 August 2010.

ACPD
12, 15049–15082, 2012

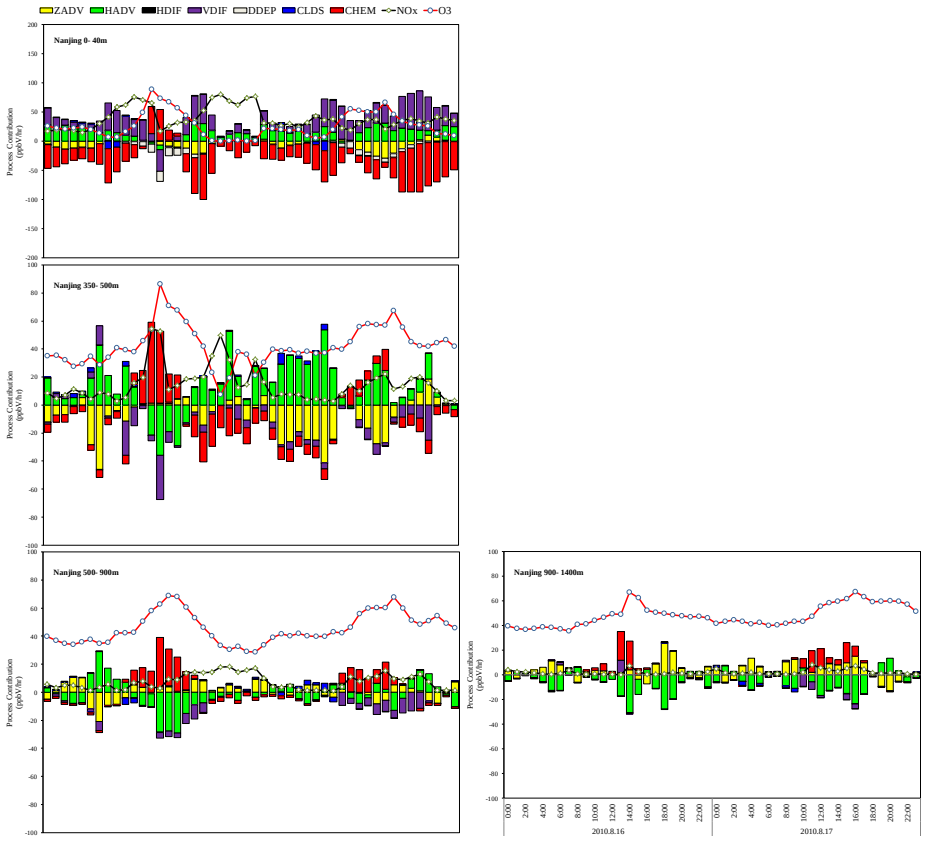

Fig. 7. Atmospheric processes contribution to net O_3 density at Nanjing site during 16–17 August 2010.

ACPD
12, 15049–15082, 2012

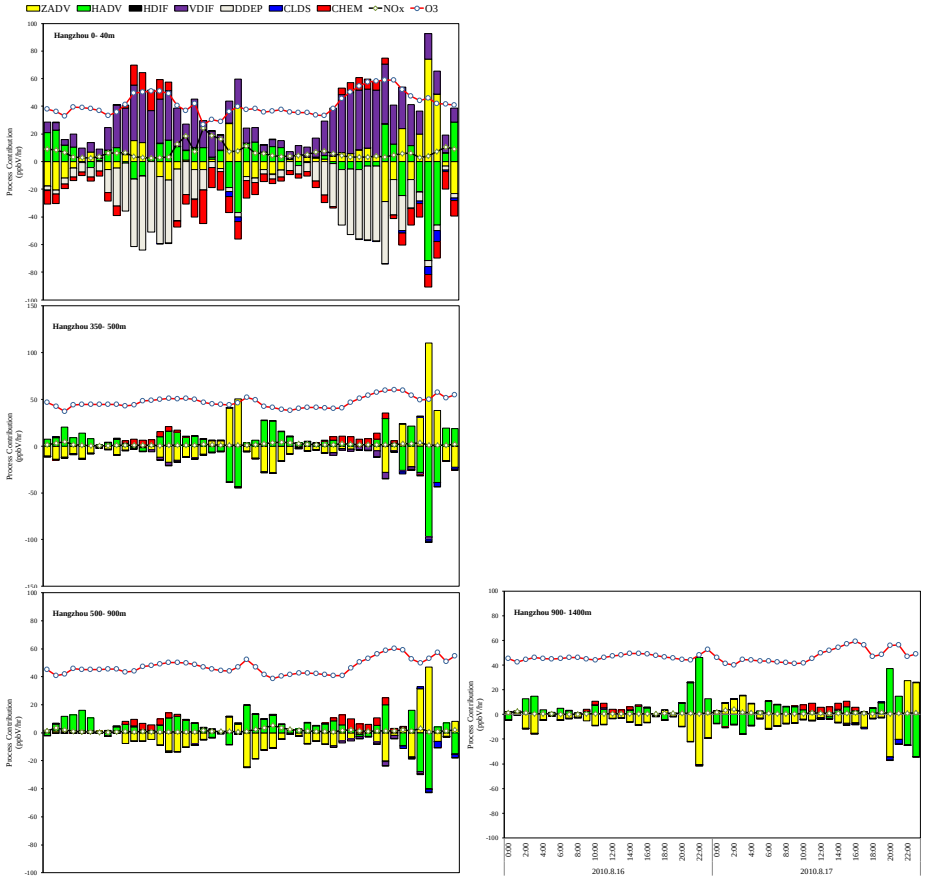

Fig. 8. Atmospheric processes contribution to net O_3 density at Hangzhou site during 16–17 August 2010.

ACPD
12, 15049–15082, 2012

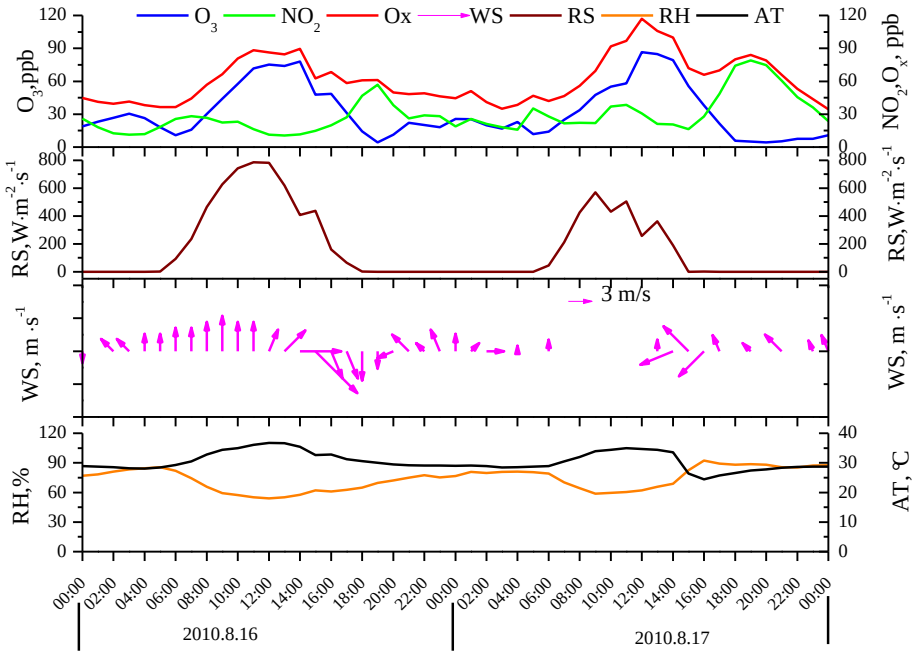

Fig. 9. Time series of meteorological conditions and mass concentrations that observed at SAES monitoring site during the high O_3 pollution episodes on 16–17 August 2010 (RS: solar radiation intensity; WS: wind speed; AT: air temperature; RH: relative humidity).

ACPD
12, 15049–15082, 2012

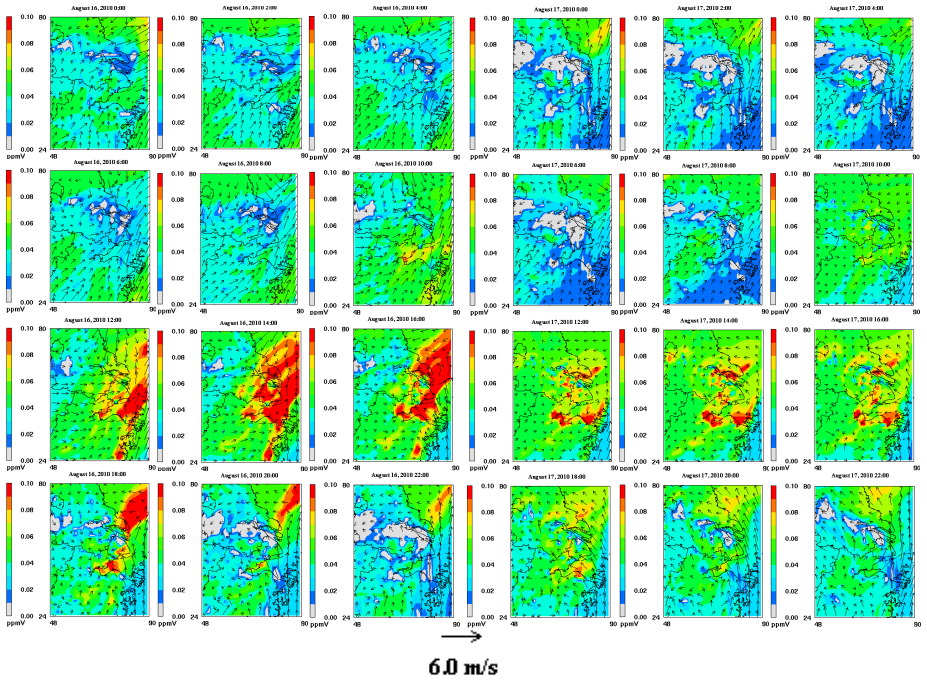

Fig. 10. Regional ozone transport during the high O_3 pollution episodes on 16–17 August 2010.

ACPD
12, 15049–15082, 2012